

PRELIMINARY LITHOGEOCHEMISTRY FOR ‘EXPLOITS DYKES’ FROM THE BADGER MAP AREA, EXPLOITS SUBZONE, CENTRAL NEWFOUNDLAND

H. Sandeman and D. Copeland¹
Mineral Deposits Section

¹Paragon Minerals Corporation, 140 Water Street, Suite 605, St. John’s, NL A1C 6H6

ABSTRACT

Since 2002, exploration in the Badger map area (NTS 12A/16) of central Newfoundland has targeted a series of turbidite-hosted orogenic quartz-vein systems. This exploration has demonstrated a significant Au resource in the Golden Promise gold prospect (Jaclyn Zone; ca. 90 000 oz contained Au) and moreover, has resulted in a substantial revision of the geology of this poorly exposed area. A significant outcome of this collective mapping is the recognition of a regionally extensive, fanning array of generally cryptic basaltic dykes that crosscut all of the major geological units of the map area.

At the Jaclyn Zone, the dykes, which comprise two distinct petrological varieties, occur in close proximity to the auriferous quartz veins. TYPE-1 dykes are most abundant, exhibit well-developed, flow-banded chill margins, are plagioclase-porphyritic and are variably carbonate-sericite altered. These dykes chill against the auriferous quartz veins but are locally cut by quartz veins and occur as fragments in minor breccia zones adjacent to the veins. These are, therefore, contemporaneous with quartz-vein emplacement and gold mineralization. TYPE-2 dykes are less abundant and comprise medium-grained (\leq 2 mm) relatively fresh, plagioclase-clinopyroxene-magnetite gabbros; these likely postdate gold mineralization and alteration.

Lithogeochemical data indicate that TYPE-1 dykes are subalkaline, tholeiitic basalts that are strongly LILE-(Th/Nb_{CN} = 2.7-4.9) and LREE-enriched (La/Yb_{CN} = 2.8-3.9); TYPE-2 dykes are alkaline to transitional alkaline tholeiitic basalts that are LILE-(Th/Nb_{CN} = 0.90-0.96) and LREE-enriched (La/Yb_{CN} = 2.7-2.9). Incompatible trace-element variations and abundances indicate TYPE-2 are likely derived from an enriched mantle source comparable in composition to E-MORB, whereas TYPE-1 dykes exhibit petrochemical indices suggesting they are Llandovery or younger magmas derived from either a moderately mature tholeiitic oceanic magmatic arc, or they are continental tholeiites.

INTRODUCTION

The Badger map area (NTS 12A/16; Figure 1) and the expansive lowlands along the Exploits River valley are heavily covered by unconsolidated glacial and fluvial deposits, and therefore have very sparse bedrock outcrop. Most of the exposed bedrock occurs along highways, river beds and, locally, along forest-access roads, hence few new exposures have been found since the work of Kean and Jayasinghe (1982). Because of the limited bedrock exposure and the poor geoscience knowledge base, the region received little attention from mineral exploration companies. In 2002, however, a forest fire razed thick brush in heavily drift-covered areas immediately southwest of the community of Badger, thereby providing easier logistical access; this resulted in the discovery of a series of new gold showings. The largest of these, the Jaclyn Zone, was discovered by prospector William Mercer, and comprised a

series of coarse-grained, comb-textured and stylolitic quartz boulders arrayed in a boulder train and exposed on subcropping, bedrock-cored ridges. Although the geology of the Golden Promise area is described elsewhere (Copeland and Newport, 2004, 2005; Pilgrim and Giroux, 2008; Sandeman *et al.*, *this volume*), one of the major outgrowths of the exploration work in the Badger map area, following the discovery of Golden Promise, was a substantial revision of the regional geology based on interpretation of airborne magnetic and resistivity data. In particular, Copeland and Newport (2004, 2005) recognized a regionally extensive, fanning array of previously cryptic basaltic dykes that crosscut all of the major geological units of the region. It is not known if these are correlative with the numerous diabase dykes recognized in the Dawes Pond map area to the north (Dickson, 2000) or in the Hodges Hill map area (NTS 02E/04) to the northeast (Dickson, 1999) of the Badger map area.

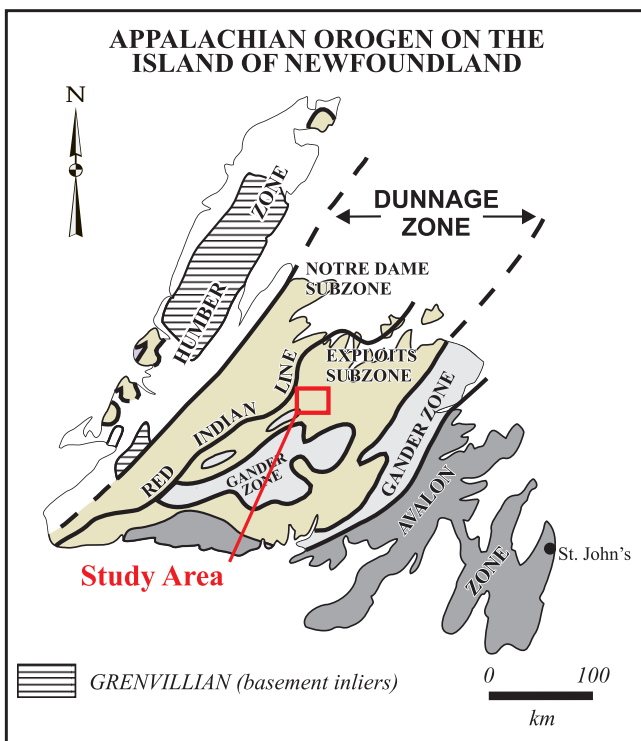


Figure 1. Location map showing the location of the Badger study area in the Dunnage Zone, central Newfoundland.

The study area lies immediately to the southeast of the tectonic boundary between the Notre Dame and Exploits subzones of the Dunnage Zone of the Appalachians. Within the Dunnage Zone, rocks of the Exploits Subzone lie to the southeast of the Red Indian Line and are considered to have peri-Gondwanan affinities. In contrast, rocks of the Notre Dame Subzone, which are of peri-Laurentian affinity, lie to the northwest of the Red Indian Line (Williams *et al.*, 1988; Williams, 1995). In the Exploits Subzone, rocks of the Cambrian–Ordovician Victoria Lake supergroup (VLSG: Evans and Kean, 2002; Rogers and van Staal, 2002) comprise, at least, three volcanic-rock dominated sequences that are stratigraphically and structurally intercalated with marine sedimentary rocks consisting of vari-coloured shales along with volcaniclastic sandstones and wackes. Many of these, particularly those of the study area, were recently assigned to the Stanley Waters Formation by Rogers *et al.* (2005). Collectively, rocks of the VLSG are conformably(?) overlain by polymictic conglomerates, medium-grained quartz-rich sandstones and sparse shaly horizons of the Badger Group. This is considered to be a continentally derived, Ordovician–Silurian overlap sequence deposited in restricted oceanic basins during closure of Iapetus Ocean (Williams and O'Brien, 1991; Williams, 1995).

Until the recent flurry of exploration activity, historical geological maps (*e.g.*, Kean and Jayasinge, 1982) indicated

that the host rocks of the Jaclyn veins composed part of the Badger Group, a unit that at the time was unnamed, but was subsequently defined by Williams (1995). In this area of poor exposure, however, modern, airborne magnetic and resistivity studies (Copeland and Newport, 2005), along with property-scale geological mapping, trench mapping and an array of 92 shallow drillholes (Pilgrim and Giroux, 2008) have significantly improved our knowledge of the 3-D architecture of the rocks of the region. These investigations have outlined persistent and continuous magnetic and conductive horizons versus poorly magnetic and non conductive horizons within the rocks. Along with key but rare, well-exposed bedrock outcrops, a more sound and informed subdivision of the distribution of rock types and a more accurate delineation of the drift-covered contacts between the VLSG and the Badger Group have been realized. The recent detailed field work and regional geophysical data has yielded new interpretive maps (Copeland and Newport, 2005) that indicate that the auriferous quartz veins of the Golden Promise area are likely hosted by upward-fining marine clastic sedimentary rocks of the upper VLSG rather than the siliciclastic flysch sequences of the Badger Group (Williams and O'Brien, 1991; Williams, 1995; Pilgrim and Giroux, 2008 and references therein).

Another highly significant outcome of this work is the recognition of a previously enigmatic, widespread array of basaltic dykes that crosscut all of the volcano-sedimentary rocks of the Badger map area. Aeromagnetic and resistivity data illustrate the presence of a series of northeast- to southeast-fanning, magnetic basaltic dykes (Figure 2) that have a probable focal point, centred on the Skull Hill syenite (Copeland and Newport, 2005). Exploration drilling on the Golden Promise property included a total of 57 intersections of mafic dykes in 98 holes from a number of widely dispersed localities (Copeland and Newport, 2004, 2005). On the basis of field observations in 2009, the areal extent of these late, postorogenic dykes has been expanded, as visually comparable dykes were observed to crosscut (with chilled margins) both co-mingled mafic–silicic granitoid rocks of the Hodges Hill pluton, as well as intermediate volcanic rocks of the Buchans Group. The composition of these dykes and their possible correlation with those described herein will be addressed in a future contribution.

INTRUSIVE RELATIONSHIPS AND DYKE PETROLOGY

Two outcrop exposures of late, crosscutting mafic dykes were observed in the Badger map area. At the Jaclyn Zone, an 8-cm-wide, near-vertical, 078°-trending carbonate-altered plagioclase porphyritic mafic dyke (sample HS08-8) was observed to crosscut green-grey siltstones at the south end of the Main trench (Plate 1). A 20-cm-wide, steeply dipping (78°), 250°-trending plagioclase-porphyritic mafic

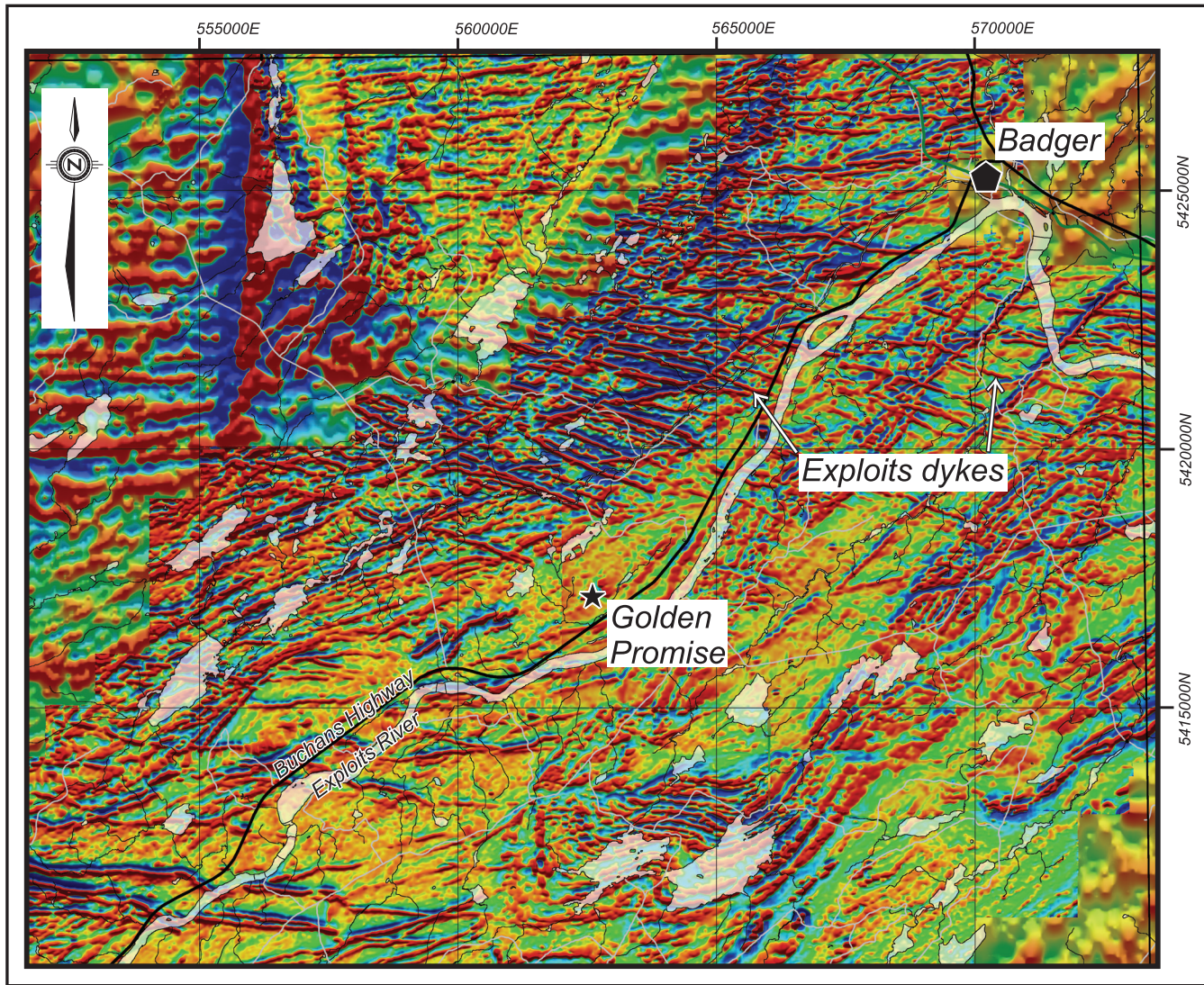


Figure 2. First vertical derivative aeromagnetic map of the Golden Promise property and westward-lying areas showing the regional expression of the east-northeast- to southeast-trending Exploits dykes (after Copeland and Newport, 2004). This is a composite image having high resolution sections over the Golden Promise area and lower resolution background.

dyke was observed to crosscut bedding in a moderately dipping sequence of medium-grained, blue-grey quartz sandstone and intercalated black mudstone rip-ups of the Badger Group, ca. 1 km east of the community of Badger on the Trans-Canada Highway (sample HS09-21B; Plate 2). The remainder of the dykes occur within exploration drillholes on the Golden Promise property.

Two distinct varieties of mafic dykes (TYPES-1 and -2) are observed in drillcore from the Golden Promise area. TYPE-1 dykes are the more abundant and typically comprise fine-grained, flow-aligned plagioclase-porphyritic basalt (Plate 3). Plagioclase phenocrysts as well as fine-grained laths in the groundmass are extensively replaced by saussurite-sericite, chlorite and carbonate (Plate 4). Pyrox-

ene or relict prismatic pseudomorphs of uralite and chlorite after pyroxene are only observed in coarser grained varieties. Opaque minerals comprise <1% and are typically anhedral grains of hematite after magnetite. Chalcopyrite and pyrite locally occur as tiny anhedral grains in the groundmass in association with acicular, skeletal hematite after magnetite. These TYPE-1 dykes exhibit complex, apparently mutual crosscutting relationships with the auriferous quartz veins. They have been noted to chill against the large, auriferous quartz veins and contain quartz fragments (Plate 5) but they have also been observed to be crosscut by quartz veins (Plate 6). An extensive review of drill logs, submitted assessment reports and observations of diamond-drill core, indicate that quartz vein and TYPE-1 mafic dyke emplacement were likely contemporaneous.



Plate 1. A ca. 8-cm-wide carbonate altered mafic dyke (078/80°) that crosscuts spotty-textured green-grey siltstones of the upper Victoria Lake supergroup (sample HS08-8).



Plate 2. A 20-cm-wide, plagioclase-porphyritic mafic dyke (250/78°: outlined in white) that cuts medium-grained, blue-grey sandstone of the Badger Group (BG: sample HS08-21B).

TYPE-2 dykes are less abundant and comprise medium-grained (≤ 2 mm) relatively fresh, plagioclase–clinopyroxene–magnetite gabbros (Plates 7 and 8). Subhedral plagioclase phenocrysts are partially saussuritized whereas anhedral to locally oikoclastic clinopyroxene is mantled by chlorite and locally biotite. Magnetite comprises both, large anhedral grains that are typically embayed and are partially replaced by hematite or, small acicular, skeletal grains that are similarly altered to hematite. These do not preserve relationships with the quartz veins, and because of their fresh character, TYPE-2 dykes are inferred to postdate gold mineralization and alteration.

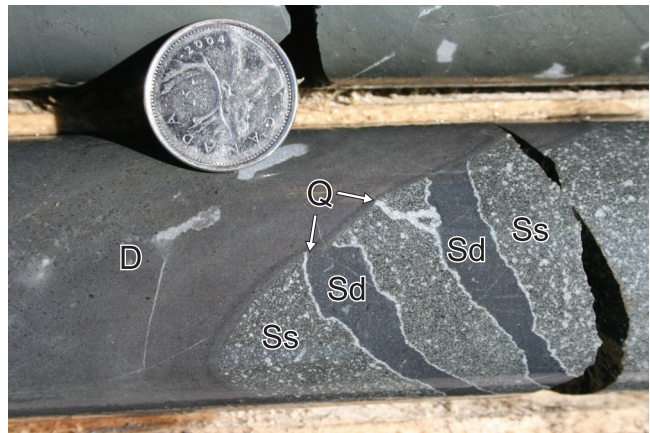


Plate 3. A flow-aligned, plagioclase-porphyritic dyke (D) (sample GP07-85_58.55m) with chill margins that cut arenitic sandstone (Ss) of the Victoria Lake supergroup. Note that the dyke cuts and chills against the sandstone as well as sandstone dykes (Sd) that cut the sandstone. These sandstone dykes have quartz-rich, silicified margins (Q) that are also truncated. Coin is 24 mm in diameter.

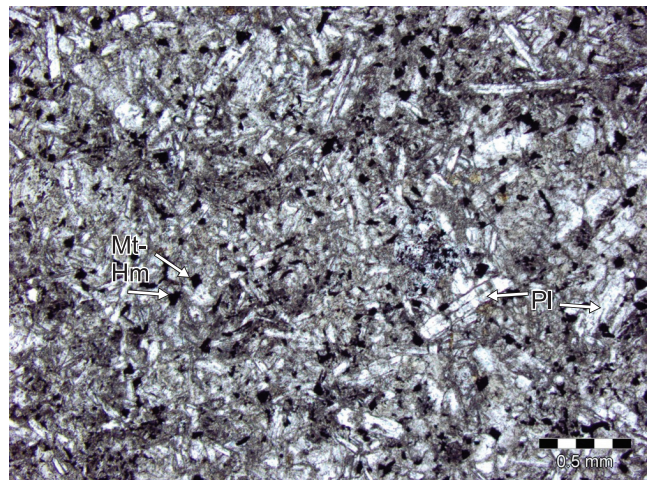


Plate 4. Photomicrograph of TYPE-1 dyke (sample GP07-80_147.9m) showing the fine-grained, chlorite–sericite–carbonate-rich groundmass with euhedral, remnant plagioclase phenocrysts (Pl) and abundant fine-grained anhedral grains of hematite replacing magnetite (Hm–Mt).

LITHOGEOCHEMISTRY

ANALYTICAL METHODS

The lithogeochemical study undertaken here characterize the compositional variations of a small number of dykes



Plate 5. A flow-aligned, chilled margin of a TYPE-1 dyke containing xenoliths of white, polycrystalline quartz (*Q*) vein material.



Plate 6. A flow-aligned, chilled margin of a TYPE-1 dyke cut by margin parallel, narrow white quartz veins. Core is 45 mm in diameter.



Plate 7. A TYPE-2 gabbroic dyke (sample GP07-82_129.3 m) having a coarse-grained interior (top) and a fine-grained chill margin (bottom). Coin is 28 mm in diameter.

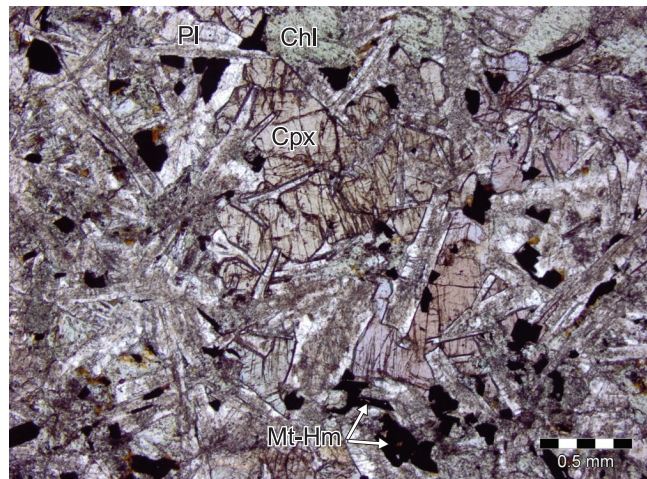


Plate 8. Photomicrograph of TYPE-2 dyke (sample GP07-82_129.3 m) having medium-grained intergrowths of anhedral, oikocrystic clinopyroxene (Cpx) with euhedral plagioclase phenocrysts (Pl). Note the pale-green chlorite (Chl) as well as abundant, anhedral opaque grains comprising hematite after magnetite (Hm–Mt) in the groundmass.

and help to provide insight into their origin. The interior of the dyke intersections were sampled, where possible, to avoid altered chill margins that may yield anomalous compositions. Samples were analyzed at the Geochemical Laboratory, Department of Natural Resources, Government of Newfoundland and Labrador, for their major and selected trace elements. Analytical methods used for these elements are after Finch (1998). The samples were also analyzed for REE and other selected elements by ICP-MS, total digestion methods at XRAL Laboratories in Ancaster, Ontario, using standard methods outlined on their website (<http://www.act-labs.com/>). Gold was determined via INAA at Bequerel Laboratories, Mississauga, Ontario (<http://www.bequerellabs.com/>). A total of 14 samples of mafic dyke from drillcore and surface were analyzed; the results are presented in Table 1. It is emphasized that, because most of the specimens were obtained from a series of drillholes intersecting a very restricted part of the dyke swarm, it is likely that these samples represent along-strike variations in only a few distinct dykes. Thus, the variability in the compositions of the dykes is likely significantly greater than demonstrated herein. Also note that many of the dykes are visibly altered and hence their whole-rock compositions may have been modified by post-crystallization fluid–rock interaction. This results in modification and mobilization of many major and mobile trace elements, but typically under most circumstances, has little effect on the immobile trace elements (Pearce and Cann, 1973; Wood *et al.*, 1979; Middelburg *et al.*, 1988). We therefore place much emphasis on the immo-

Table 1. Lithogeochemical data for mafic dykes from the Badger map area. All oxides are in weight % whereas trace elements are in ppm. UTM coordinates in NAD27, zone 21 format. Key: VLSG = inferred Victoria Lake supergroup (*cf.* Sandeman *et al.*, *this volume*); BG = Badger Group; FeO^T = total iron as ferrous iron; < = below the given detection limit; Mg# = molecular (MgO/MgO+FeO^T)*100; CN subscript denotes chondrite normalized ratios. Please note that many of the dykes were taken from diamond-drill holes and hence their UTM coordinates reflect the collar locations and not the surface projection of the dyke.

Sample	GP07-80	GP07-82	GP07-85	GP07-85	GP07-88	GP07-88	GP07-89	GP07-92	HS08-8	HS08-	HS08-	GP07-80	GP07-81	GP07-82
	147.9m	144.4m	104.26m	58.55m	108.7m	93.2m	61.9m	108.75m	21B	21B*	106.4m	129.4m	129.3m	
Host unit	VLSG	BG	BG	VLSG	VLSG	VLSG								
Type	TYPE-1	TYPE-2	TYPE-2	TYPE-2										
easting	562685	562835	562202	562202	562336	562336	562270	562465	562248	571485	571485	562685	562787	562835
northing	5417076	5417093	5417092	5417092	5417090	5417090	5417123	5417193	5417134	5424883	5424883	5417076	5417080	5417093
SiO ₂	47.97	49.47	50.22	50.04	49.55	47.19	48.49	46.01	44.13	48.36	48.00	45.29	44.98	44.91
TiO ₂	1.50	1.58	1.56	1.51	1.54	1.42	1.48	1.62	1.42	1.68	1.71	1.91	2.16	2.03
Al ₂ O ₃	15.23	15.53	15.63	15.50	15.26	14.88	15.06	15.87	13.98	16.55	16.55	16.23	16.67	15.95
FeO ^T	8.12	8.47	8.40	8.51	8.27	8.10	8.01	8.51	7.77	8.88	8.86	9.94	10.16	10.48
Fe ₂ O ₃	0.61	0.92	1.26	1.00	1.21	0.76	0.98	0.78	0.70	1.18	1.11	1.69	1.21	1.44
FeO	7.57	7.65	7.27	7.62	7.19	7.41	7.13	7.81	7.14	7.82	7.86	8.43	9.07	9.18
MnO	0.14	0.16	0.15	0.17	0.16	0.19	0.16	0.43	0.17	0.16	0.16	0.18	0.31	0.17
MgO	6.75	7.04	6.95	7.15	6.75	6.72	6.67	3.96	6.21	6.04	5.66	8.36	7.62	8.34
CaO	8.01	7.20	7.06	7.88	7.42	6.89	7.91	7.62	6.58	6.84	6.99	8.40	7.13	7.22
Na ₂ O	1.98	2.64	2.63	2.25	2.13	1.92	2.31	0.10	0.66	2.95	2.70	2.49	2.85	3.14
K ₂ O	0.64	1.25	1.45	1.10	1.76	0.93	0.69	3.04	3.38	1.15	1.08	0.68	1.19	1.00
P ₂ O ₅	0.24	0.24	0.24	0.24	0.24	0.23	0.24	0.26	0.22	0.25	0.26	0.28	0.31	0.29
CO ₂	3.99	1.30	0.91	0.42	1.11	4.03	3.52	6.34	9.81	1.34	2.14	0.58	0.57	0.53
S	0.12	0.14	0.11	0.14	0.04	0.02	0.14	0.13	0.02	0.31	0.17	0.14	0.36	0.12
LOI	6.90	4.15	3.76	3.16	4.03	8.03	6.73	10.63	12.82	4.16	5.30	3.20	4.26	3.98
Total	98.37	98.69	98.99	98.46	98.03	97.40	98.64	99.00	98.19	98.02	98.27	98.06	98.77	98.68
Mg#	59.70	59.70	59.59	59.95	59.27	59.66	59.75	45.38	58.74	54.79	53.23	59.96	57.21	58.64
Cr	167	156	156	176	164	145	156	183	109	128	134	157	160	161
Ni	108	105	104	115	105	103	102	111	100	56	56	119	106	114
Co	35	36	36	37	37	36	37	29	38	42	43	82	48	46
Sc	24.3	25.6	25.5	25.4	25.1	22.2	24.0	25.9	22.6	31.9	32.3	24.2	30.9	29.1
V	182	174	173	175	182	178	178	201	168	235	244	206	231	220
Cu	32	33	32	31	38	32	32	32	34	35	31	40	46	39
Pb	3	3	2	7	5	7	<1	<1	7	<1	<1	<1	<1	<1
Zn	73	75	74	74	74	72	72	71	83	79	83	82	95	81
Cd	0.3	<0.1	<0.1	0.2	<0.1	0.3	0.3	0.4	0.3	0.1	0.3	0.4	<0.1	<0.1
Ag	<0.5	<0.5	<0.5	<0.5	<0.5	<0.5	<0.5	<0.5	<0.5	<0.5	0.7	12.5	<0.5	<0.5
Sb	2.9	2.9	5.1	7.5	5	79.4	2.1	2.4	10.5	<0.2	1	1.8	5.5	3
Sn	7	<1	11	17	13	3	2	1	<1	<1	9	3	4	21
Tl	0.3	0.29	0.28	0.23	0.85	0.2	0.31	0.23	1.14	0.3	0.29	0.85	0.42	0.24
W	<0.5	<0.5	0.9	0.6	1.6	1.6	<0.5	<0.5	<0.5	<0.5	1.3	<0.5	0.7	0.5
As	<2	<2	<2	<2	15	36	11	74	63	7	27	<2	9	<2
Be	0.4	0.5	0.5	0.5	0.7	0.4	1.5	0.9	0.6	0.5	0.4	0.7	0.5	0.5
Bi	<0.1	<0.1	0.2	0.1	0.2	<0.1	<0.1	<0.1	<0.1	<0.1	<0.1	<0.1	<0.1	<0.1
Cs	4.6	1.5	1.2	0.7	1	1.1	2.4	2.2	1.8	0.7	0.7	9.8	1.7	2.8
Ga	16	16	17	16	17	16	16	15	15	17	18	29	19	17
Ge	1.3	1.3	1.5	2.4	1.5	1.2	1.2	1	1.6	1.1	1.4	2.4	1.7	1.3
Li	50.0	23.7	30.2	38.4	30.0	36.7	24.6	35.3	23.0	45.5	53.3	18.1	32.8	39.1
Ba	236	1225	1179	395	795	195	290	265	459	605	468	114	787	630
Rb	28	26	29	26	46	27	18	69	99	36	31	50	29	25
Sr	336	424	546	356	393	259	303	121	278	645	584	579	449	598
Hf	2.9	2.8	3.2	3.1	3.3	3.2	3	2.4	2.6	3	3.2	5.4	3.9	3.6
Ta	0.32	0.31	0.34	0.31	0.33	0.33	0.33	0.29	0.3	0.28	0.3	0.76	0.52	0.48
Nb	4.3	4.3	4.6	4.3	4.5	4.6	4.6	4.1	4.3	4.3	4.7	10.3	6.8	6.5
Y	24.4	24.9	26.9	23.8	26.1	24.8	25.4	26	22.6	25.8	27.9	45.2	30.1	28.3
Zr	113	115	124	120	129	137	123	101	112	126	133	252	169	157
Th	2.32	2.24	2.64	2.13	2.59	2.54	2.58	1.30	2.15	1.88	2.05	1.09	0.77	0.71
U	0.73	0.71	0.83	0.68	0.85	0.77	0.81	0.46	0.68	0.59	0.57	0.41	0.25	0.26
La	11.20	11.20	12.20	11.00	12.10	12.10	12.10	10.00	10.90	13.90	15.00	16.90	10.70	10.10

Table 1. (Continued)

Sample	GP07-80	GP07-82	GP07-85	GP07-85	GP07-88	GP07-88	GP07-89	GP07-92	HS08-8	HS08-	HS08-	GP07-80	GP07-81	GP07-82
Host unit	147.9m	144.4m	104.26m	58.55m	108.7m	93.2m	61.9m	108.75m	21B	21B*	106.4m	129.4m	129.3m	
Type	TYPE-1	TYPE-2	TYPE-2	TYPE-2										
easting	562685	562835	562202	562202	562336	562336	562270	562465	562248	571485	562685	562787	562835	
northing	5417076	5417093	5417092	5417092	5417090	5417090	5417123	5417193	5417134	5424883	5424883	5417076	5417080	5417093
Ce	26.40	26.40	28.50	25.70	28.10	28.40	28.20	24.70	25.50	32.40	34.80	43.80	28.50	26.40
Pr	3.85	3.86	4.16	3.75	4.09	3.79	4.05	3.64	3.66	4.55	4.57	6.69	4.41	4.12
Nd	16.10	15.70	16.70	15.40	16.40	16.10	16.80	15.60	14.60	17.90	18.00	28.50	18.40	17.30
Sm	3.89	3.88	4.24	3.77	4.12	4.05	4.05	3.92	3.56	4.24	4.54	7.35	4.78	4.46
Eu	1.34	1.41	1.45	1.30	1.39	1.58	1.39	1.31	1.21	1.29	1.28	2.76	1.83	1.71
Gd	4.26	4.34	4.56	4.15	4.44	4.47	4.53	4.48	4.00	4.68	4.88	8.37	5.30	4.90
Tb	0.70	0.71	0.77	0.68	0.75	0.72	0.71	0.74	0.64	0.75	0.80	1.31	0.88	0.82
Dy	4.19	4.26	4.55	4.06	4.54	4.34	4.34	4.44	3.85	4.48	4.84	7.78	5.28	4.89
Ho	0.87	0.88	0.94	0.85	0.94	0.91	0.94	0.94	0.84	0.94	1.03	1.62	1.09	1.00
Er	2.76	2.75	2.95	2.64	2.88	2.78	2.86	2.79	2.55	2.83	3.18	4.89	3.31	3.13
Tm	0.41	0.41	0.43	0.40	0.41	0.40	0.41	0.42	0.37	0.40	0.47	0.70	0.48	0.45
Yb	2.39	2.43	2.61	2.34	2.58	2.47	2.52	2.54	2.22	2.53	2.81	4.21	2.80	2.67
Lu	0.35	0.36	0.38	0.33	0.38	0.36	0.38	0.37	0.32	0.37	0.39	0.61	0.42	0.38
(La/Yb) _{CN}	3.36	3.31	3.35	3.37	3.36	3.51	3.44	2.82	3.52	3.94	3.83	2.88	2.74	2.71
(La/Sm) _{CN}	1.86	1.86	1.86	1.88	1.90	1.93	1.93	1.65	1.98	2.12	2.13	1.48	1.45	1.46
(Gd/Yb) _{CN}	1.47	1.48	1.45	1.47	1.42	1.50	1.49	1.46	1.49	1.53	1.44	1.64	1.57	1.52
Eu/Eu*	1.01	1.05	1.01	1.00	0.99	1.14	0.99	0.96	0.98	0.89	0.83	1.08	1.11	1.12
(Th/La) _{CN}	1.69	1.63	1.77	1.58	1.75	1.72	1.74	1.06	1.61	1.11	1.12	0.53	0.59	0.57
(La/Nb) _{CN}	2.70	2.70	2.75	2.66	2.79	2.73	2.73	2.53	2.63	3.36	3.31	1.70	1.63	1.61
(Th/Nb) _{CN}	4.58	4.42	4.87	4.20	4.88	4.68	4.76	2.69	4.24	3.71	3.70	0.90	0.96	0.93

bile trace elements including the high field strength elements (HFSE) and the rare earth elements (REE).

CLASSIFICATION AND GEOCHEMICAL VARIATIONS

All the dykes are basalts in terms of both, major (LeBas *et al.*, 1986) and incompatible trace-element data (Pearce, 1996; Figure 3A). They are generally subalkaline, tholeiitic basalts exhibiting FeO^T and TiO_2 enrichment with fractionation, however, TYPE-2 dykes fall on, and above, the alkaline–subalkaline dividing line of De la Roche *et al.* (1980; Figure 3B) and appear to be transitional to mildly alkaline. TYPE-1 dykes are characterized by variable SiO_2 and K_2O , reflected in a K_2O versus SiO_2 diagram (Figure 3C; Pecerillo and Taylor, 1976) where two particularly strongly carbonate- and sericite-altered dykes have mildly lower silica but significantly elevated K_2O , high enough to qualify these as medium- K_2O , calc-alkaline basalts even though they exhibit tholeiitic compositions. These 2 samples are also characterized by elevated CO_2 , As and Rb and have lower Na_2O relative to the remaining TYPE-1 dykes. None of the analyzed dykes contained anomalous Au, with all samples yielding values of <2 ppb.

The results of the incompatible trace-element paleotectonic plots (*cf.* Pearce and Cann, 1973; Wood *et al.*, 1979) are somewhat ambiguous, although distinction between the two dyke suites are clear; TYPE-2 dykes have elevated Zr,

Nb, Hf and Y and strongly depleted Th relative to TYPE-1 dykes (see Figure 4). Incompatible element variations in the dykes are examined using REE and multi-element plots, normalized to chondrite (CN) and mid-ocean ridge basalt (N-MORB), respectively (normalizing values from Sun and McDonough, 1989). Figure 5A shows the REE patterns for the 14 dykes, and Figure 5B, the extended multi-element plots for the same samples. TYPE-1 dykes have very consistent, mutually parallel REE patterns. Exceptions are the duplicate analyses of the dyke that crosscut the Badger Group (sample HS08-21B; Plate 2). This dyke has more strongly fractionated LREE $(\text{La}/\text{Sm})_{\text{CN}} = 2.12\text{--}2.13$ vs. 1.65–1.98, a modest negative europium anomaly expressed as Eu/Eu* (0.83–0.89 vs. 0.96–1.14; after Taylor and McClenan, 1985) and has the highest heavy REE (HREE) abundances. TYPE-2 dykes also exhibit mutually parallel REE patterns but exhibit greater variations in REE abundances. These have flat La–Ce–Pr segments with $(\text{La}/\text{Sm})_{\text{CN}} = 1.45\text{--}1.48$, Eu/Eu* = 1.08–1.12 and HREE abundances higher than all TYPE-1 dykes.

Figure 6 further outlines the compositional affinities of the dykes and suggests plausible paleotectonic settings for their primary magma generation. TYPE-1 dykes have elevated Th/Yb, Th/Nb with corresponding high $(\text{La}/\text{Sm})_{\text{CN}}$ and $(\text{La}/\text{Yb})_{\text{CN}}$ relative to TYPE-2 dykes (Figure 6). They plot between the fields for basaltic rocks from the Mariana arc (Elliot *et al.*, 1997) and that for central Andean calk-alkaline basalts (Feeley and Davidson, 1994; Sandeman, 1995). This

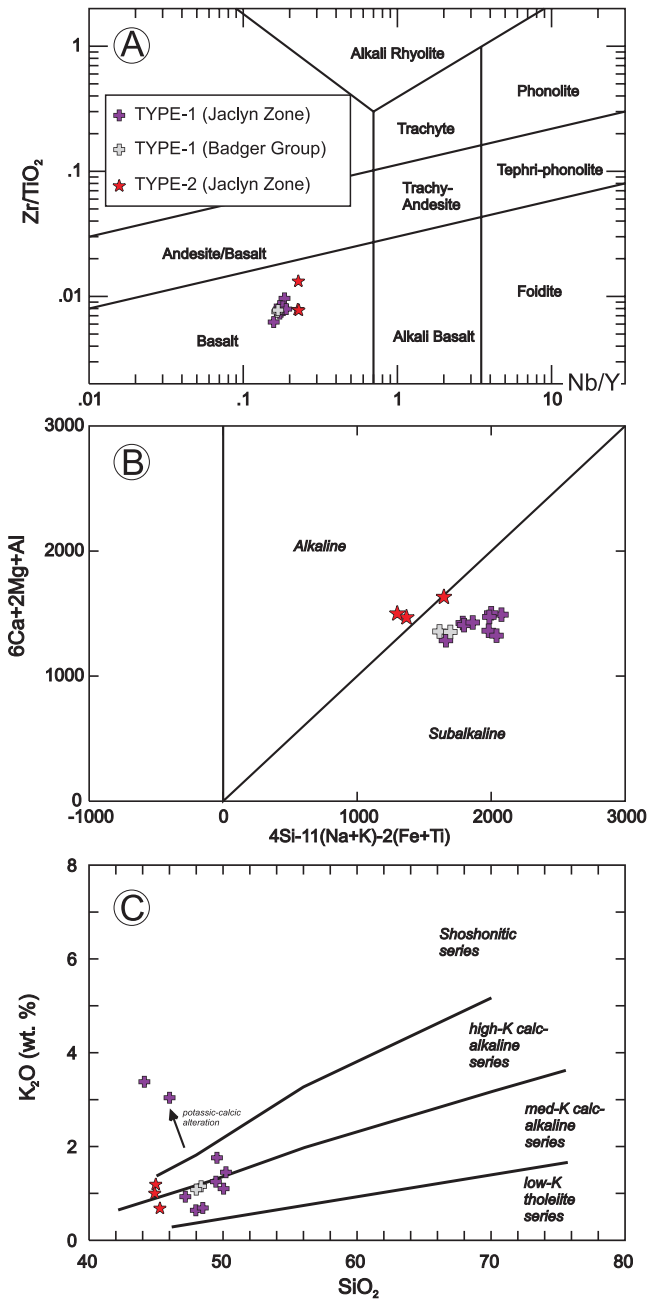


Figure 3. A) Zr/TiO_2 vs Nb/Y discrimination diagram after Pearce (1996; modified from Winchester and Floyd, 1977) showing the compositions of the dykes. B) Major oxide, R1-R2 cation plot of De la Roche et al. (1980) showing the sub-alkaline nature of the TYPE-1 dykes and the weakly alkaline compositions of the TYPE-2 dykes. C) K_2O vs SiO_2 plot (after Peccerillo and Taylor, 1976; Rickwood, 1989) demonstrating the medium- to high- K_2O nature of the dykes and the significant increase in K_2O resulting from strong sericite–carbonate alteration.

compositional space is occupied by evolved oceanic-arc basalts and transitional calc-alkaline basalts (Bau and Knit-

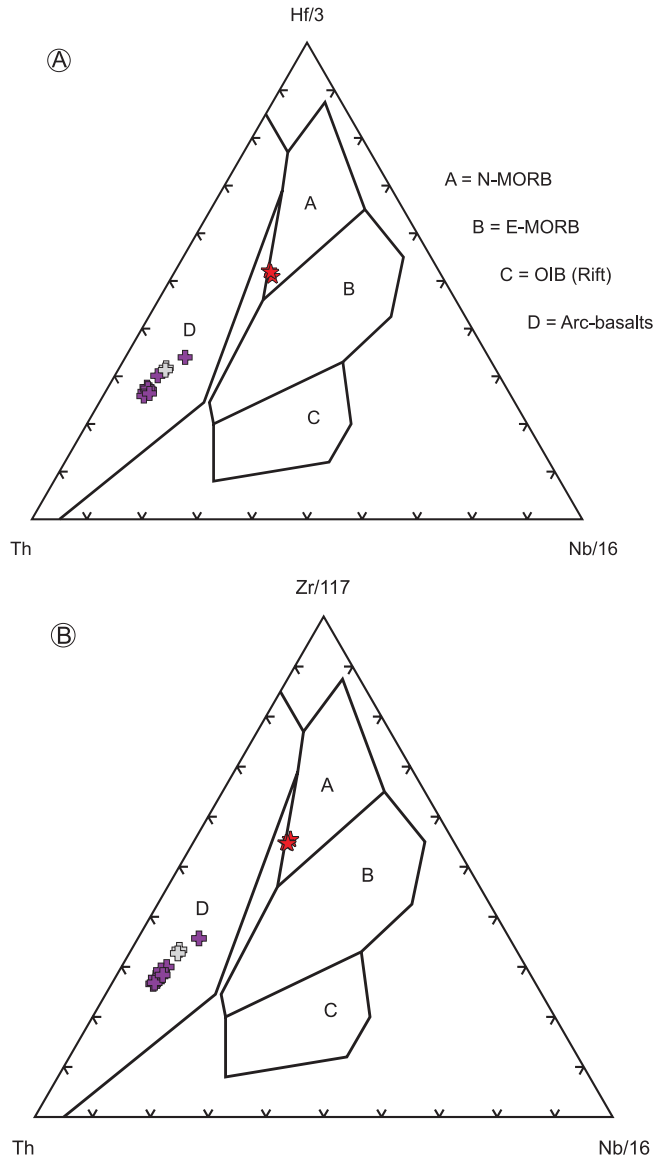


Figure 4. Paleotectonic discrimination diagrams. A) Ternary plot of incompatible elements (Th–Hf–Nb; Wood et al., 1979) suggesting a volcanic arc origin for the TYPE-1 dykes and an enriched, N-MORB origin for the TYPE-2 dykes. B) Ternary plot of incompatible elements (Th–Zr–Nb; Wood et al., 1979) suggesting a volcanic arc origin for the TYPE-1 dykes and an enriched, NMORB origin for the TYPE-2 dykes. Symbols as in Figure 3.

tel, 1993), however, it is also the compositional locus of numerous, low- TiO_2 continental tholeiitic basalt suites as represented by mafic sills and dykes of the western Canadian Gunbarrel magmatic event (Sandeman et al., 2007; Ootes et al., 2008). TYPE-2 basalts are most similar to EM-TYPE (enriched MORB) basalts but have mildly elevated Th/Nb ratios. Such variable Th–Nb–La relationships, clearly shown in Figure 5B, have commonly been attributed to modest crustal contamination of variably enriched (relative

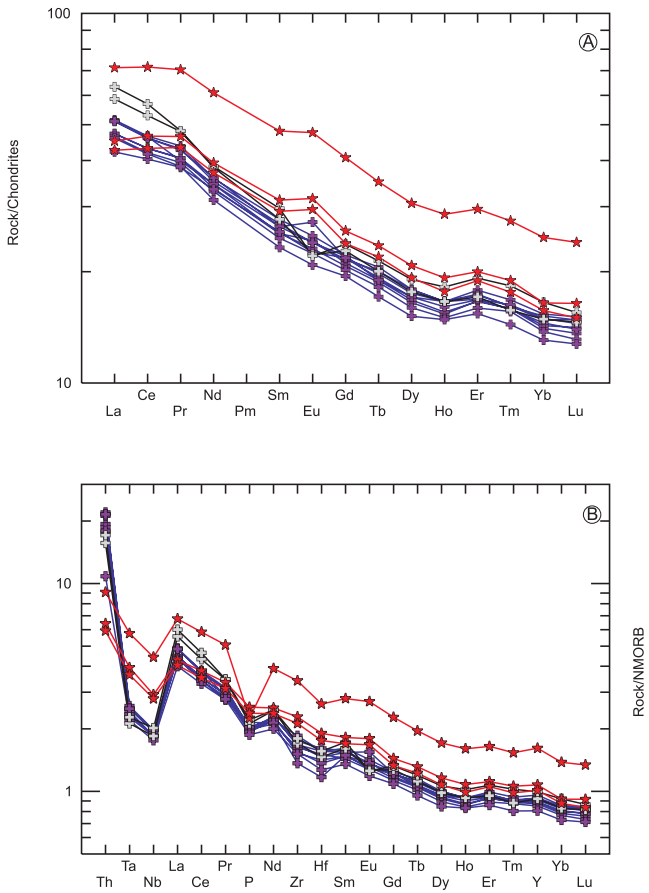


Figure 5. A) Chondrite normalized (Sun and McDonough, 1989) rare-earth-element patterns for dykes from the Badger map area. B) Primitive-mantle-normalized (PM: Sun and McDonough, 1989) multi-element plot for dykes from the Badger map area. Symbols as in Figure 3.

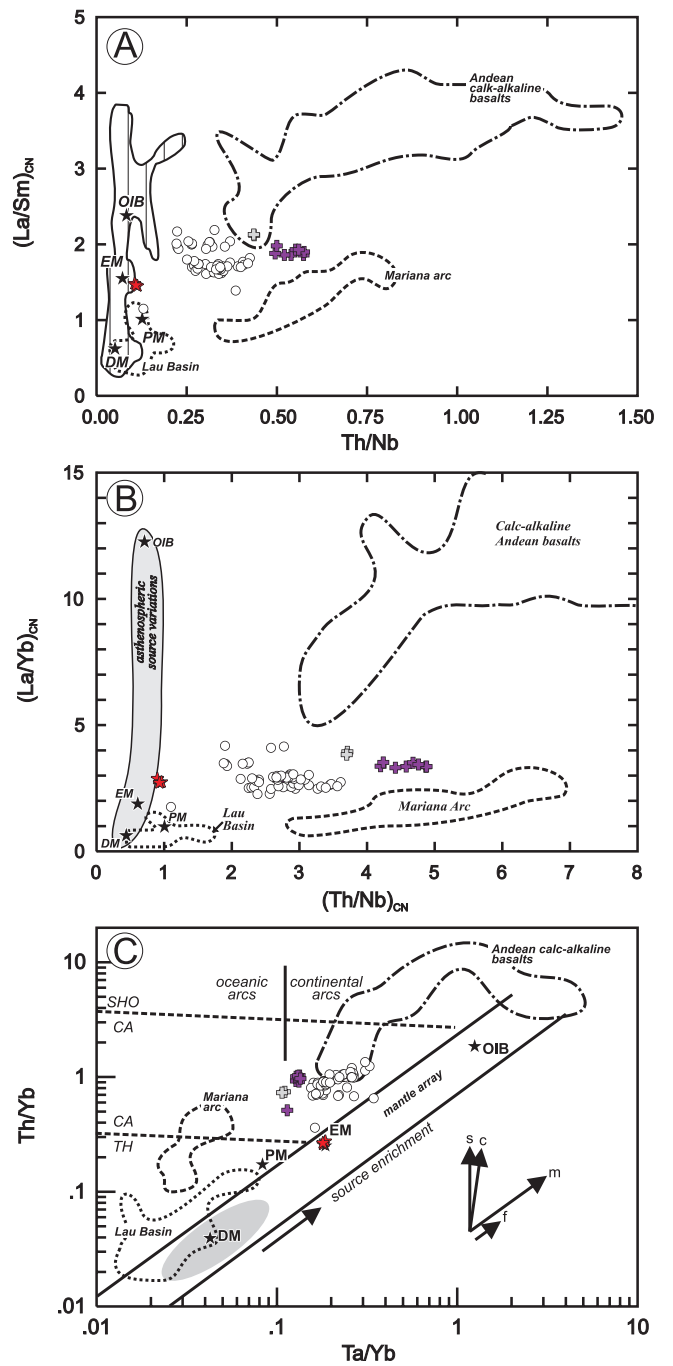


Figure 6. (top opposite) Incompatible element ratio plots for dykes from the Badger map area. A) A plot of $(La/Sm)_{CN}$ vs Th/Nb (after Elliott et al., 1997) demonstrating the Th -enriched nature of TYPE-1 dykes vs TYPE-2 dykes and the cospatial mantle array. B) A plot of $(La/Yb)_{CN}$ vs $(Th/Nb)_{CN}$ demonstrating the mildly enriched LREE abundances of the dykes and similarly emphasizing the Th -enriched nature of the TYPE-1 dykes. C) A plot of Th/Yb vs Ta/Yb (log scale, after Pearce, 1982) demonstrating that TYPE-2 dykes are comparable to EM-type mantle and plot within the mantle array. Note that in all of these diagrams, TYPE-1 dykes have characteristics of mature tholeiitic oceanic arc basalts

(cf. Mariana arc: Pearce et al., 1994), but also plot cospatially with many low- Ti continental tholeiite suites (open circles) exemplified by the Gunbarrel continental tholeiites of the western Canadian basin (Sandeman et al., 2007; Ootes et al., 2008). Symbols as in Figure 3. Key: black stars represent mantle end member compositions (Sun and McDonough, 1989); labelled trajectories in C represent the effects of: s - subduction; c - crustal contamination; m - mantle source variation; f - ca. 50% fractional crystallization of olivine+clinopyroxene+plagioclase.

to N-MORB) mantle-derived melts (Barrie *et al.*, 1993; Gribble *et al.*, 1998; Hollings, 2002). A possible geotectonic setting for their derivation may be an extended, or rifted magmatic arc such as the Northern Mariana trough (Gribble *et al.*, 1998) or the Sea of Japan (Pouclet *et al.*, 1994).

CONCLUSIONS

Field, drillhole and petrographic data suggest that 2 distinct suites of relatively young basaltic dykes crosscut Ordovician–Silurian volcanosedimentary rocks of the VLSG and the Badger Group. Reconnaissance investigations in 2009 confirm that visually comparable dykes also crosscut granitoids of the Hodges Hill pluton as well as volcanic rocks of the Buchans Group.

One of the dykes discussed herein cuts quartz sandstones of the Badger Group. Graptolitic fossils in the Badger Group constrain its depositional age to early Ashgill to latest Llandovery (Williams and O'Brien, 1991; O'Brien, 2003), indicating that the TYPE-1 dykes must be younger than *ca.* 430 Ma (International Commission on Stratigraphy, 2009). Furthermore, if the mafic dykes observed to crosscut the Hodges Hill granite are correlative, then collectively the TYPE-1 dykes must be younger than 415 Ma, a Rb–Sr isochron age that presently is the best estimate of the age of that intrusion (415.6 ± 2.1 Ma; Moore, 1984).

The most abundant dykes (TYPE-1) exhibit complex, mutually crosscutting relationships with auriferous quartz veins at the Golden Promise prospect. They are fine-grained, plagioclase porphyritic, always exhibit well-developed, commonly flow-aligned chill margins and, are often extensively Fe-carbonate and potassically altered. TYPE-2 dykes are less abundant, are invariably fresh relative to TYPE-1 dykes and, although they apparently have comparable trends and perhaps utilize similar crustal fractures or conduits, they have not yet been observed in contact with the mineralized veins. Observed relationships strongly suggest that the TYPE-1 dykes were emplaced contemporaneous with the auriferous quartz veins, whereas TYPE-2 dykes are apparently younger, and postdate mineralization and alteration.

TYPE-1 dykes are subalkaline tholeiitic basalts characterized by LILE and LREE-enrichment and are either K₂O-enriched (hydrothermal alteration affect) oceanic arc-basalts laterally emplaced from a distal, westward-lying volcanic centre, or they may represent a suite of late orogenic continental tholeiites of unknown affinity. TYPE-2 dykes are transitional alkaline basalts having modest LILE and LREE enrichment and exhibiting variable LILE/HFSE ratios (*e.g.*, Th/Nb and La/Nb) and may represent a postorogenic magmatic gasp from a modestly enriched (EM?) mantle source. Future work will attempt to incorporate ⁴⁰Ar–³⁹Ar and U–Pb (baddeleyite?) geochronology, further lithogeochemistry and

radiogenic tracer isotopic studies (Sm–Nd, Rb–Sr) to better characterize their age, the nature of their magmatic source(s) and the processes that may have modified their compositions since their formation.

ACKNOWLEDGMENTS

Paragon Minerals Corporation and Crosshair Exploration and Mining Corporation are thanked for access to their drillholes and databases. Gerry Kilfoil graciously provided the aeromagnetic map. Andy Kerr is thanked for commenting on an earlier version of this contribution. Peter Valley kindly reviewed the paper.

REFERENCES

- Barrie, C.T., Ludden, J.N. and Green, T.H.
1993: Geochemistry of volcanic rocks associated with Cu–Zn and Ni–Cu deposits in the Abitibi subprovince. *Economic Geology*, Volume 88, pages 1341–1358.
- Bau, M. and Knittel, U.
1993: Significance of slab-derived partial melts and aqueous fluids for the genesis of tholeiitic and calc-alkaline island-arc basalts: evidence from Mt. Arayat, Philippines. *Chemical Geology*, Volume 105, pages 233–251.
- Copeland, D.A. and Newport, A.
2004: Assessment report on prospecting, rock and soil sampling, trenching, airborne geophysics and diamond drilling on the Golden Promise property, central Newfoundland. NTS 12A/16 and 02D/13. [NFLD/2902]
- 2005: Supplementary 2nd year assessment report on soil sampling, prospecting, geological mapping, trenching and diamond drilling on the Golden Promise property, central Newfoundland [NFLD/2910]
- De la Roche, H., Leterrier, J., Grandclaude, P. and Marchal, M.
1980: A classification of volcanic and plutonic rocks using R1R2-diagram and major element analyses – its relationships with current nomenclature. *Chemical Geology*, Volume 29, pages 183–210.
- Dickson, W.L.
1999: Geology of the Hodges Hill (NTS 2E/04) map area, north-central Newfoundland. *In Current Research, Newfoundland Department of Mines and Energy, Geological Survey, Report 99-1*, pages 317–342.
- 2000: Geology of the eastern portion of the Dawes Pond (NTS 12H/1) map area, central Newfoundland. *In Current Research, Newfoundland Department of Mines*

- and Energy, Geological Survey, Report 2000-1, pages 127-145.
- Evans, D.T.W. and Kean, B.F.
2002: The Victoria Lake Supergroup, central Newfoundland – its definition, setting and volcanogenic massive sulphide mineralization. Open File NFLD/2790, 80 pages.
- Feeley, T.C. and Davidson, J.P.
1994: Petrology of calc-alkaline lavas at Volcan Ollagie and the origin of compositional diversity at Central Andean stratovolcanoes. *Journal of Petrology*, Volume 35, pages 1295-1340.
- Finch, C.J.
1998: Inductively coupled plasma-emission spectrometry (ICP-ES) at the Geochemical Laboratory. In *Current Research*. Newfoundland Department of Mines and Energy, Geological Survey, Report 98-1, pages 179-193.
- Gribble, R.F., Stern, R.J., Newman, S., Bloomer, S.H. and O'Hearn, T.
1998: Chemical and isotopic composition of lavas from the northern Mariana trough: implications for magma genesis in back-arc basins. *Journal of Petrology*, Volume 39, pages 125-154.
- Hollings, P.
2002: Archean Nb-enriched basalts in the northern Superior Province. *Lithos*, Volume 64, pages 1-14.
- International Commission on Stratigraphy (ICS)
2009: International Stratigraphic Chart (<http://www.stratigraphy.org/>).
- Kean B.F. and Jayasinge, N.R.
1982: Geology of the Badger map area (12A/16), Newfoundland. Newfoundland Department of Mines and Energy, Mineral Development Division, Report 81-2, 37 pages.
- LeBas, M.J., LeMaitre, R.W., Streckeisen, A. and Zanettin, B.
1986: A chemical classification of volcanic rocks based on the total alkali silica diagram. *Journal of Petrology*, Volume 27, pages 745-750.
- Middelburg, J.J., Van der Weijden, C.H. and Woittiez, J.R.W.
1988: Chemical processes affecting the mobility of major, minor and trace elements during weathering of granitic rocks. *Chemical Geology*, Volume 68, pages 253-273.
- Moore, P.V.
1984: The geochemistry and petrogenesis of the Hodges Hill granite – Twin Lakes diorite complex. Unpublished B.Sc (Hons) thesis, Memorial University of Newfoundland, St. John's, Newfoundland. 51 pages. [NFLD/2675].
- O'Brien, B.
2003: Geology of the central Notre Dame Bay region (parts of NTS areas 2E/3,6,11), northeastern Newfoundland. Newfoundland Department of Mines and Energy, Geological Survey, Report 03-3, 147 pages.
- Ootes, L., Sandeman, H.A., Lemieux, Y. and Leslie, C.
2008: The 780 Ma Tsezotene Sills, Mackenzie Mountains: a field, petrographical, and geochemical study. NWT Open Report 2008-11, 21 pages and appendices.
- Pearce, J.A.
1982: Trace element characteristics of lavas from destructive plate boundaries. In *Andesites*. Edited by R.S. Thorpe. John Wiley and Sons, pages 525–548.
1996: A user's guide to basalt discrimination diagrams. In *Trace Element Geochemistry of Volcanic Rocks; Applications for Massive Sulphide Exploration*. Short Course Notes, Geological Association of Canada, Volume 12, pages 79-113.
- Pearce, J.A. and Cann, J.R.
1973: Tectonic setting of basic volcanic rocks determined using trace element analyses. *Earth and Planetary Science Letters*, Volume 19, pages 290-300.
- Pearce, J.A., Ernewein, M., Bloomer, S.H., Parson, L.M., Murton, B.J. and Johnson, L.E.
1994: Geochemistry of Lau Basin volcanic rocks: influence of ridge segmentation and arc proximity. In *Volcanism Associated with Extension at Consuming Plate Margins*. Edited by J.L. Smellie. Geological Society of London, Special Publication 81, pages 53-75.
- Peccerillo, A. and Taylor, S.R.
1976: Geochemistry of Eocene calc-alkaline volcanic rocks from the Kastamonu Area, northern Turkey. Contributions to Mineralogy and Petrology, Volume 58, pages 53-61.
- Pilgrim, L.R. and Giroux, G. H.
2008: Form 43-101F1 technical report for the Golden Promise, south Golden Promise and Victoria Lake properties – Badger, Grand Falls, Buchans and Victoria Lake areas (NTS 12A/06, 09, 10, 15, 16 and 02D/13), Newfoundland and Labrador. SEDAR filing.

- Pouclet, A., Lee, J., Vidal, P., Cousens, B. and Bellon, H.
1994: Cretaceous to Cenozoic volcanism in South Korea and in the Sea of Japan: magmatic constraints on the opening of the back-arc basin. *In Volcanism Associated with Extension at Consuming Plate Margins. Edited by J.L. Smellie.* Geological Society of London, Special Publications 81, pages 169-191.
- Rickwood, P.C.
1989: Boundary lines within petrologic diagrams which use oxides of major and minor elements. *Lithos*, Volume 22, pages 247-263.
- Rogers, N. and van Staal, C.
2002: Toward a Victoria Lake Supergroup: a provisional stratigraphic revision of the Red Indian to Victoria Lakes area, central Newfoundland. *In Current Research. Newfoundland Department of Mines and Energy, Geological Survey, Report 02-1*, pages 185-195.
- Rogers, N., van Staal, C. and McNicoll, V.J.
2005: Geology, Badger, Newfoundland and Labrador. Geological Survey of Canada, Open File 4546, scale 1:50,000.
- Sandeman, H.A.I.
1995: Lithostratigraphy, petrology and geochronology of the Crucero Supergroup, Puno, SE Peru: Implications for the Cenozoic geodynamic evolution of the Southern Peruvian Andes. Unpublished Ph.D. thesis, Queen's University, Kingston, Canada, 382 pages.
- Sandeman, H.A., Ootes, L. and Jackson, V.
2007: Field, petrographic and petrochemical data for the Faber sill: petrogenesis of a “Gunbarrel Event” sill in the Wopmay Orogen, NWT, Canada. NWT Open Report 2007-7, 25 pages.
- Sandeman H.A., Rafuse, H. and Copeland, D.
This volume: The setting of orogenic, auriferous quartz veins at the Golden Promise prospect, central Newfoundland and observations on the veining and wall-rock alteration.
- Sun, S.S. and McDonough, W.F.
1989: Chemical and isotopic systematics of oceanic basalts: implications for mantle composition and processes. *In Magmatism in the Ocean Basins. Edited by A.D. Saunders and M.J. Norry.* Geological Society of London, Special Publication 42, pages 313-345.
- Williams, H.
1995: Chapter 4 – Middle Paleozoic rocks. *In Geology of the Appalachian-Caledonide Orogen in Canada and Greenland. Edited by H. Williams.* Geological Survey of Canada, Geology of Canada, Series No. 6, pages 315-446.
- Williams, H., Colman-Sadd, S.P. and Swinden, H.S.
1988: Tectonic-stratigraphic subdivisions of Central Newfoundland. *In Current Research, Part B. Geological Survey of Canada, Paper 88-1B*, pages 91-98.
- Williams, S.H. and O'Brien, B.H.
1991: Silurian graptolites from the Bay of Exploits, north-central Newfoundland and their geological significance. *Canadian Journal of Earth Sciences*, Volume 28, pages 1534-1540.
- Winchester, J.A. and Floyd, P.A.
1977: Geochemical discrimination of different magma series and their differentiation products using immobile elements. *Chemical Geology*, Volume 20, pages 325-343.
- Wood, D.A., Joron, J.L. and Treuil, M.
1979: A re-appraisal of the use of trace elements to classify and discriminate between magma series erupted in different tectonic settings. *Earth and Planetary Science Letters*, Volume 50, pages 326-336.

Note: Geological Survey file numbers are included in square brackets.